UNCLASSIFIED
~~CONFIDENTIAL~~

Copy No. 5

RM No. L8H16

NACA RM No. L8H16

CLASSIFICATION CHANGED OCT 31 1948

To UNCLASSIFIED

By authority of H. L. Dryden Date Nov. 26, 1952
per NACA Release form #1349.
By HAR 12-24-52.

NACA

RESEARCH MEMORANDUM

AERODYNAMIC CHARACTERISTICS OF A THREE-BLADE PROPELLER HAVING NACA 10-(3)(08)-03 BLADES

By

Robert E. Davidson

Langley Aeronautical Laboratory
Langley Field, Va.

NATIONAL ADVISORY COMMITTEE FOR AERONAUTICS

WASHINGTON
October 29, 1948

~~CONFIDENTIAL~~
UNCLASSIFIED

NATIONAL ADVISORY COMMITTEE FOR AERONAUTICS

RESEARCH MEMORANDUM

AERODYNAMIC CHARACTERISTICS OF A THREE-BLADE PROPELLER HAVING NACA 10-(3)(08)-03 BLADES

By Robert E. Davidson

SUMMARY

Data obtained in tests of a 10-foot diameter, three-blade propeller, having NACA 10-(3)(08)-03 blades, conducted in the Langley 16-foot high-speed tunnel are presented. The propeller performance quantities related by the tests are thrust, torque, efficiency, and advance ratio for various rotational speeds or stream Mach numbers with blade angle as a parameter. Advance Mach numbers varied from 0.12 to 0.64.

INTRODUCTION

The National Advisory Committee for Aeronautics has completed a broad program of propeller aerodynamic tests to determine the effect of varying the solidity, camber, thickness, shank form, and blade number.

The purpose of the tests discussed herein was to show the effect of varying the number of blades in a propeller. For this purpose the test results may be compared with those in reference 1 which describes similar tests of a two-blade propeller using blades identical with those in the three-blade propeller.

TESTS

The tests were conducted at various tunnel velocities for constant values of propeller rotational speed and blade angle. (See table I for summary of tests.) The fixed rotational speeds were 1140, 1350, 1500, 1600, 2000, and 2160 rpm. The blade angles at the three-quarter radius ranged from 20° to 55° in 5° increments.

A few tests at $\beta_{0.75R} = 45^{\circ}$ were made at constant Mach number for various rotational speeds from the speed which gave approximately zero torque to that which required the maximum available dynamometer torque. The dynamometer torque limitation required some of the constant Mach number tests to be terminated before peak efficiency had been reached.

APPARATUS

The tests were conducted in the Langley 16-foot high-speed tunnel with the 2000-horsepower propeller dynamometer and related equipment described in reference 1.

Propeller configuration.- The propeller configuration was as follows:

Number of blades 3
Diameter, feet 10.05
NACA blade designation . . . . 10-(3)(08)-03

Blades.- The blades were designed at the NACA Langley Laboratory and are designated NACA 10-(3)(08)-03. While the number of blades in the subject propeller was three, the blades were designed for use on a four-blade propeller. Blade-form curves are given in figure 1. The blades are characterized by the following data for the section at the 0.7 radius:

Design lift coefficient 0.3
Thickness ratio 0.08
Blade solidity. 0.03

REDUCTION OF DATA

A complete description of the method of measuring thrust, torque, rotational speed, and airspeed is given in reference 1. From these quantities the propeller coefficients were determined. Propeller thrust as used herein is propeller shaft tension with spinner force removed.

SYMBOLS

b	blade chord, feet
c_{l_d}	design section lift coefficient
C_P	power coefficient $\left(P/\rho n^3 D^5\right)$
C_T	thrust coefficient $\left(T/\rho n^2 D^4\right)$
D	propeller diameter, feet
h	blade-section maximum thickness, feet

J	advance ratio (V/nD)
M	Mach number
M_t	helical tip Mach number $\left(M\sqrt{1+\left(\frac{\pi}{J}\right)^2}\right)$
n	propeller rotational speed, rps
T	propeller thrust, pounds
V	velocity of advance, feet per second
β	blade angle, degrees
$\beta_{0.75R}$	blade angle at three-fourths tip radius, degrees
η	propeller efficiency $\left(\frac{C_T}{C_P}J\right)$

RESULTS

Faired curves of propeller performance are presented in figures 2 to 9. Test points are shown on the curves giving thrust and power coefficient.

Shown on the propeller-efficiency curves are plots of stream and helical tip Mach number as a function of J. Small discontinuities in the Mach number curves for the individual tests appeared in the data. These discontinuities, caused by changes in atmospheric conditions between periods of tunnel operation, have been faired out to show a continuous variation of Mach number with J.

Envelope-efficiency curves are plotted in figure 2 as a function of advance ratio for various rotational speeds. Also shown in figure 2 is the induced efficiency of a propeller with the Betz loading and the same disk power loading as the subject propeller operating at the envelope-efficiency advance ratio for each blade angle tested at 1350 rpm. The efficiency of this ideal propeller was obtained from the charts of reference 2 and is labeled optimum efficiency in figure 2.

DISCUSSION

Remarks on blade number and solidity.- Figure 10 shows peak efficiency at $\beta_{0.75R} = 45^\circ$ plotted against tip Mach number for three propellers differing in solidity and blade number. As the advance ratio for peak efficiency is substantially the same for the three propellers, figure 10 indicates the effect of varying blade number or solidity.

The propellers have the following characteristics at the 0.7 radius:

Propeller	Design C_L	Solidity
10-(3)(08)-03 2 blades	0.3	.060
10-(3)(08)-045 2 blades	.3	.090
10-(3)(08)-03 3 blades	.3	.090

The curve for the propeller with two 10-(3)(08)-03 blades compared with that for the propeller with two 10-(3)(08)-045 blades shows the decrease in efficiency resulting from increasing disk power loading (or, in this case, power coefficient) by increasing solidity.

The results for the propeller with two 10-(3)(08)-045 blades compared with those for the propeller with three 10-(3)(08)-03 blades show the increase in efficiency resulting from increasing the number of blades for a given set of design conditions, that is, scale, advance ratio, and power coefficient. Actually, the two-blade propeller operated at a power coefficient slightly less than that of the three-blade propeller which would mean that the difference in efficiency would have been greater than is indicated by figure 10 if the power coefficients had been equal. The trend indicated by this comparison is in agreement with theory which indicates that for optimum propellers an increase in the number of blades will increase efficiency under given design conditions (advance ratio and power coefficient held constant).

The addition of one more identical blade to a two-blade propeller results in a decrease in efficiency, however, because the effect of increasing disk power loading more than balances the tendency of the efficiency to be increased by an increase in blade number. (See curves for the propellers with two 10-(3)(08)-03 blades and with three 10-(3)(08)-03 blades in fig. 10.)

<u>The effect of compressibility on peak efficiency and power coefficient at the design blade angle</u>.- Figure 10 shows the effect of compressibility on peak efficiency at $\beta_{0.75R} = 45^{\circ}$.

Figure 11 shows the effect of compressibility on the power coefficient for the propeller with three 10-(3)(08)-03 blades and the propeller with two 10-(3)(08)-03 blades at $\beta_{0.75R} = 45^{\circ}$. This figure indicates the considerable difference in tip Mach number at which major changes in power coefficient occur for a two-blade propeller as compared with a three-blade propeller under the condition of identical blades for both propellers. The comparison is made on the basis of peak efficiency for both propellers. The comparative magnitudes of the power coefficients for the two propellers are not to be considered important because, while peak efficiency tends to be insensitive to small variations in J, power coefficient changes rapidly with J.

Langley Aeronautical Laboratory
National Advisory Committee for Aeronautics
Langley Field, Va.

REFERENCES

1. Corson, Blake W., Jr., and Maynard, Julian D.: The NACA 2000-Horsepower Propeller Dynamometer and Tests at High Speed of an NACA 10-(3)(08)-03 Two-Blade Propeller. NACA RM No. L7L29, 1948.

2. Crigler, John L., and Talkin, Herbert W.: Charts for Determining Propeller Efficiency. NACA ACR No. L4I29, 1944.

3. Solomon, William: Aerodynamic Characteristics at High Speeds of a Two-Blade NACA 10-(3)(062)-045 Propeller and of a Two-Blade NACA 10-(3)(08)-045 Propeller. NACA RM No. L8E26, 1948.

TABLE I

SUMMARY OF TESTS

Figure	Tunnel speed	Propeller speed (rpm)	Blade angle $\beta_{0.7R}$ (deg)							
3	Vary	1140		25	30	35	40	45	50	55
4	Vary	1350	20	25	30	35	40	45	50	
5	Vary	1500						45		
6	Vary	1600	20	25	30	35	40	45		
7	Vary	2000	20	25	30	35				
8	Vary	2160	20	25	30					
9(a)	M = 0.56	Vary						45		
9(b)	M = 0.60	Vary						45		
9(c)	M = 0.64	Vary						45		

NACA

[redacted]

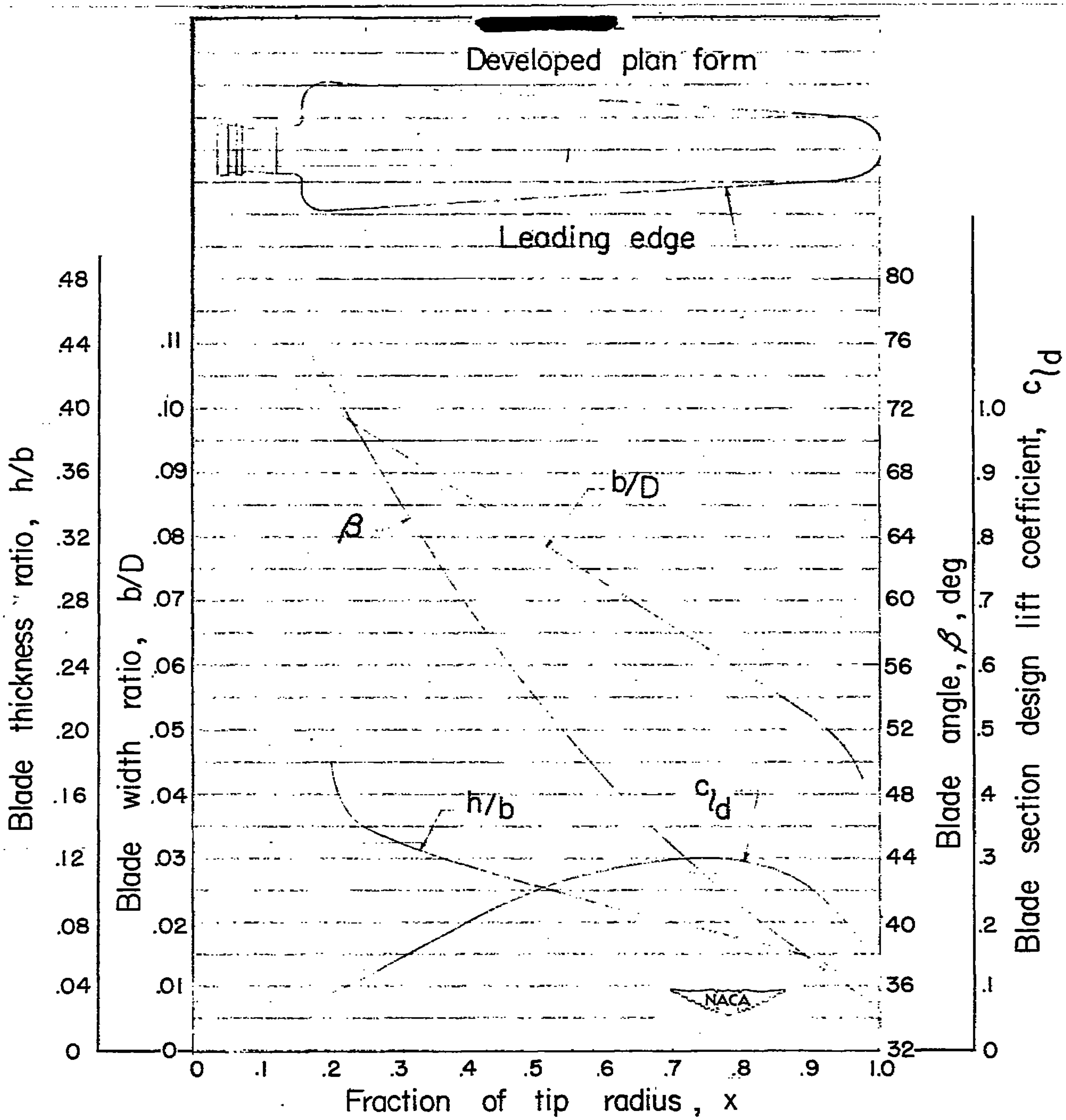

[redacted]

Figure 1.- NACA 10-(3)(08)-03 blade-form curves.

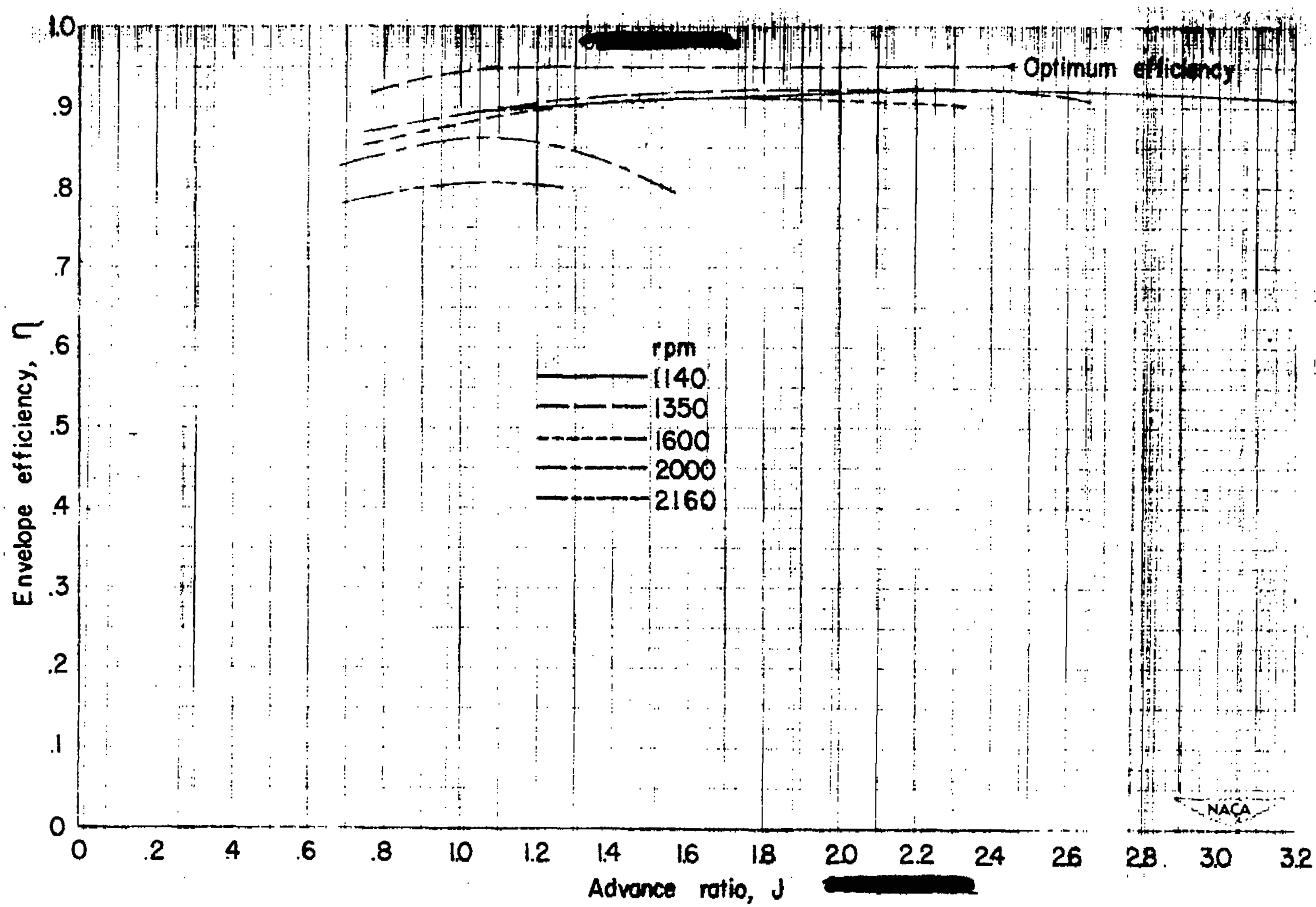

Figure 2.- Envelope efficiency of three-blade propeller with NACA 10-(3)(08)-03 blades.

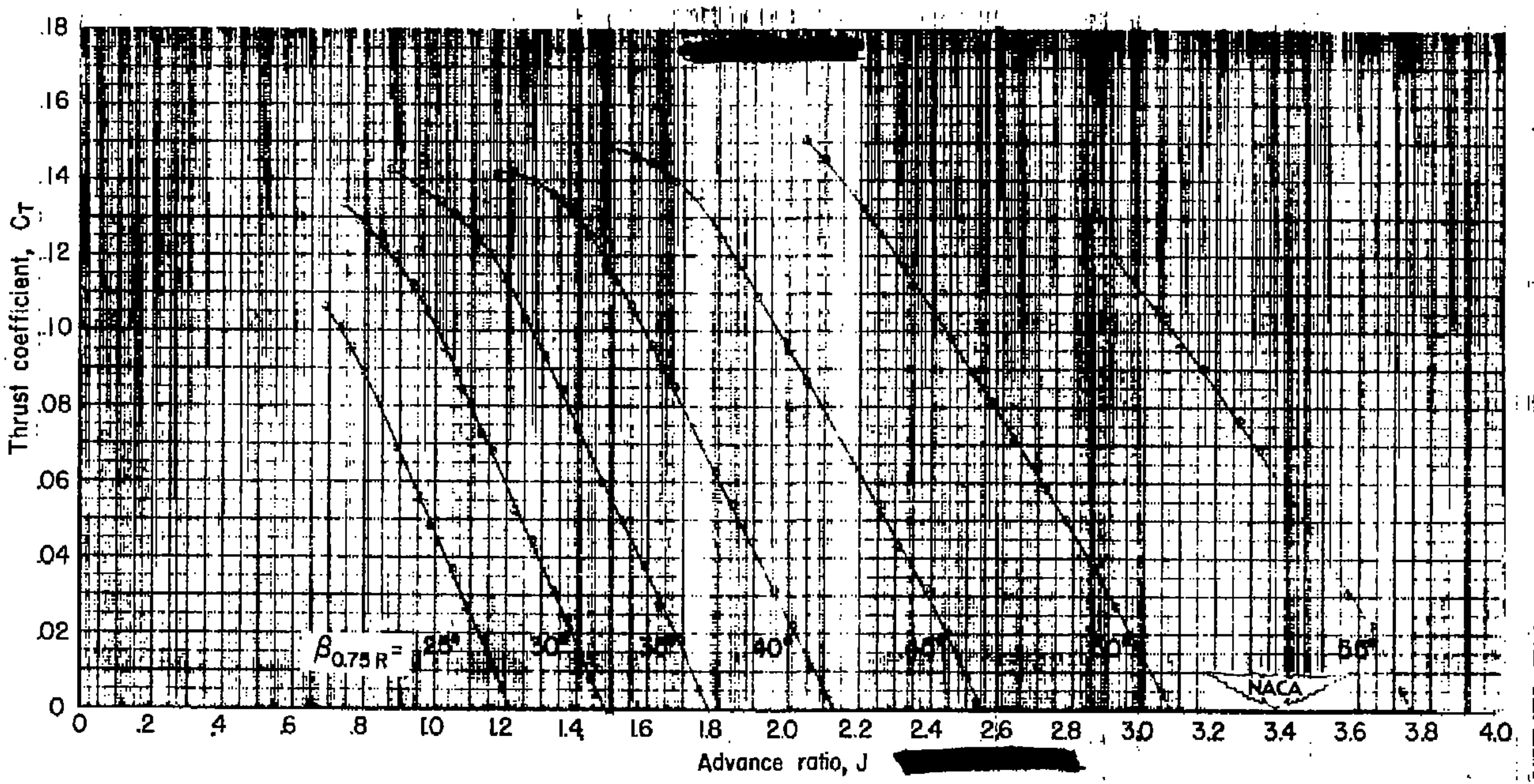

(a) Thrust coefficient.

Figure 3.- Characteristics of three-blade propeller with NACA 10-(3)(08)-03 blades. Rotational speed, 1140 rpm.

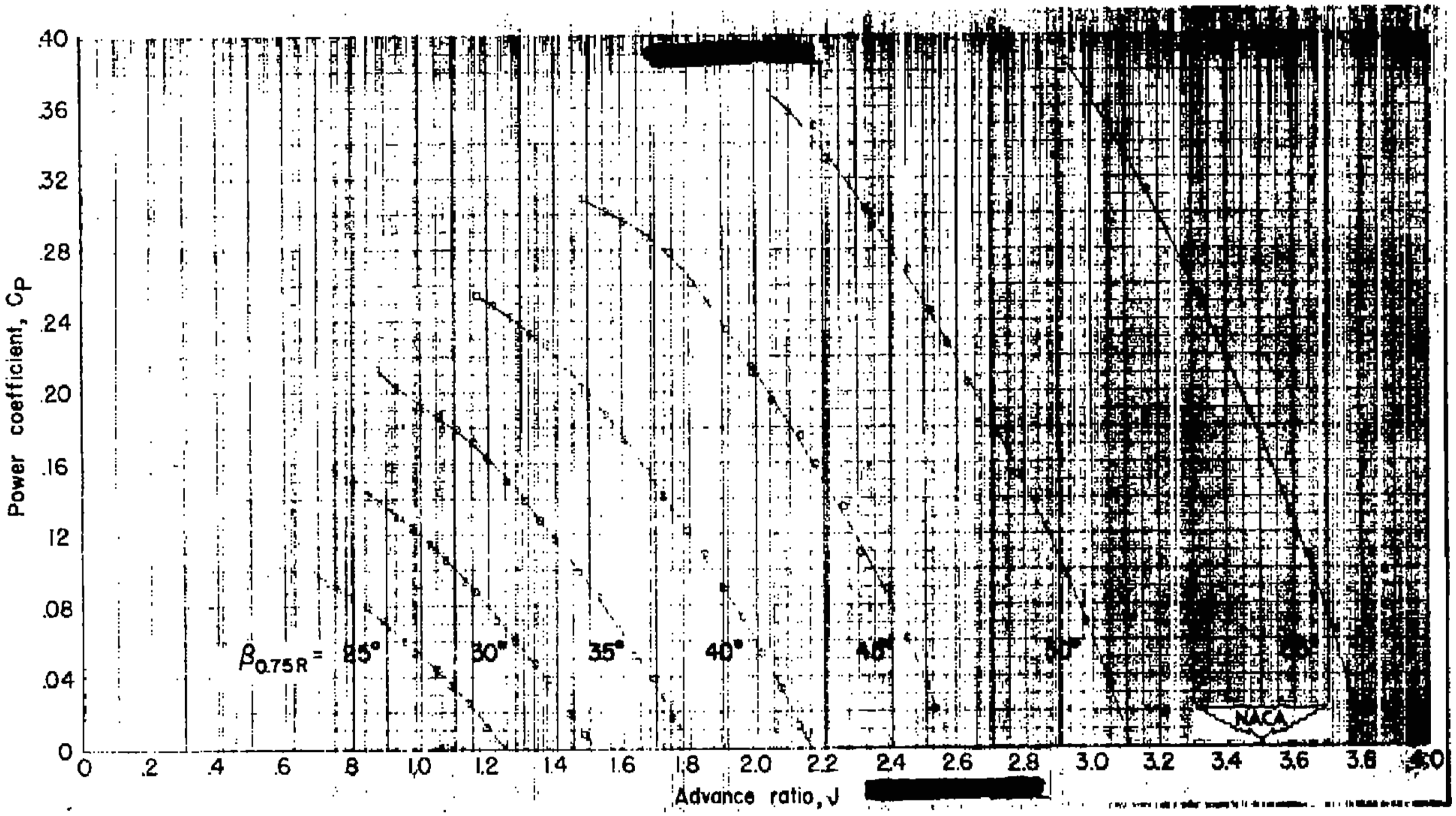

(b) Power coefficient.

Figure 3.- Continued. Rotational speed, 1140 rpm.

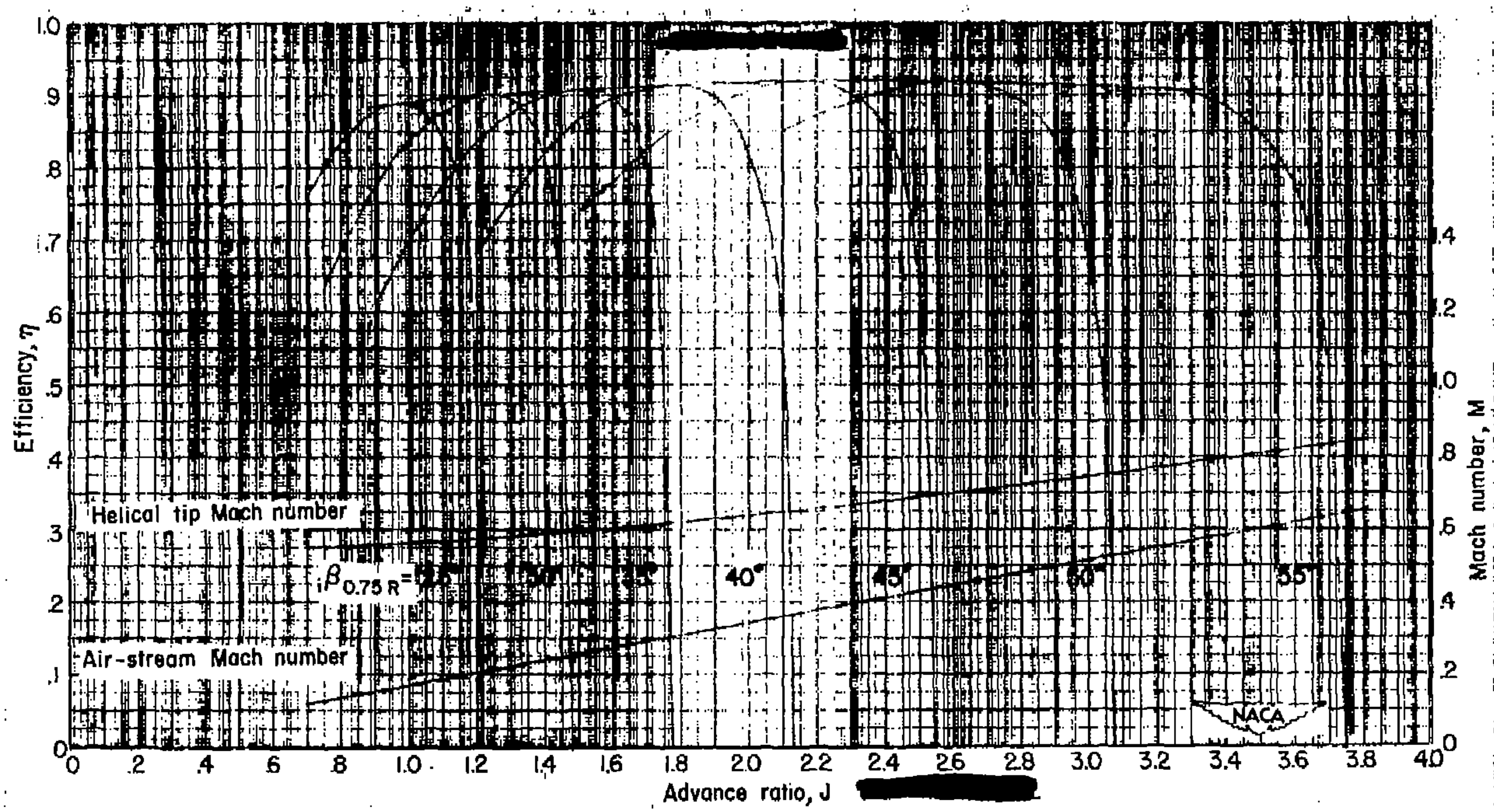

(c) Efficiency.

Figure 3.- Concluded. Rotational speed, 1140 rpm.

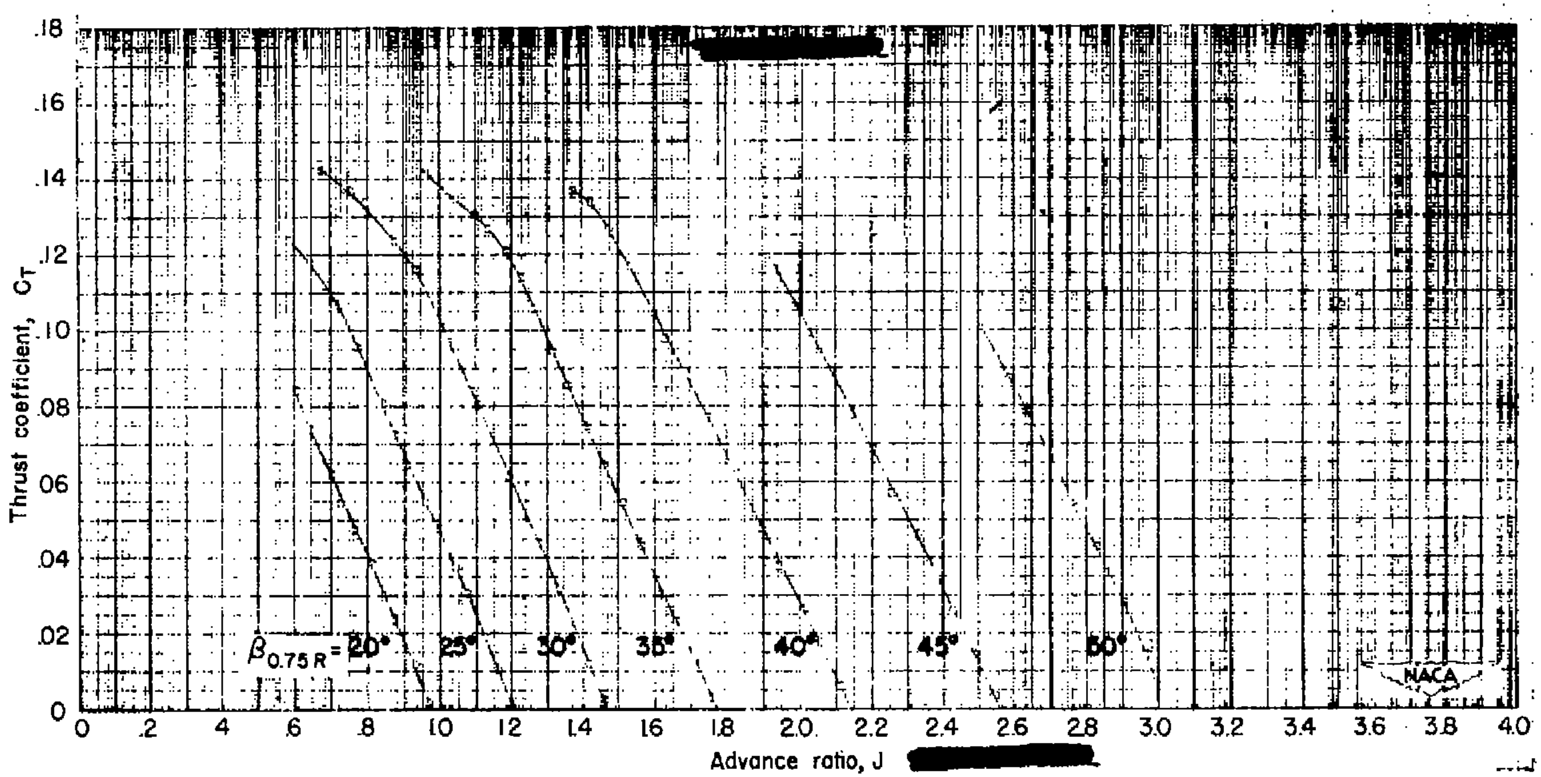

(a) Thrust coefficient.

Figure 4.- Characteristics of three-blade propeller with NACA 10-(3)(08)-03 blades. Rotational speed, 1350 rpm.

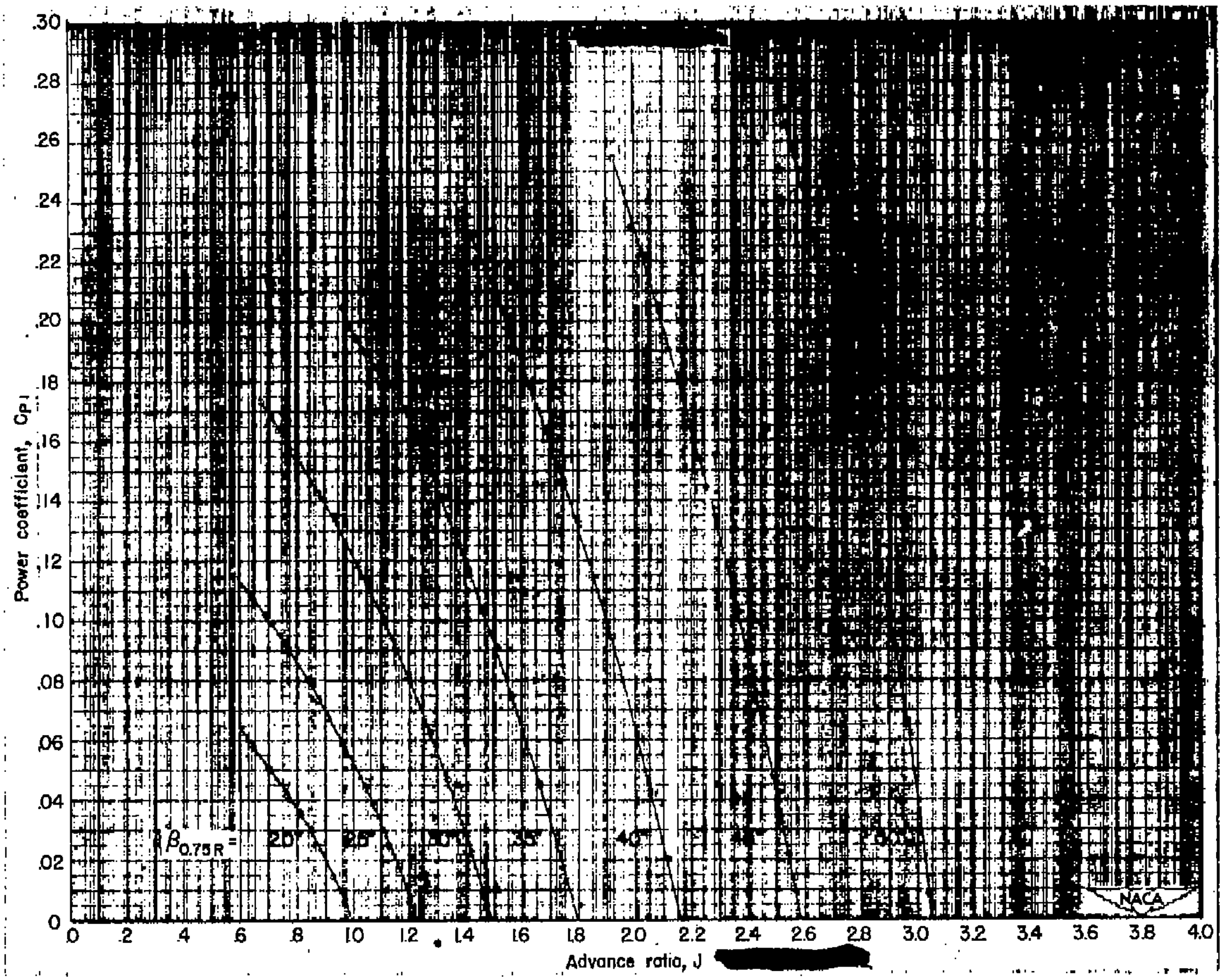

(b) Power coefficient.

Figure 4.- Continued. Rotational speed, 1350 rpm.

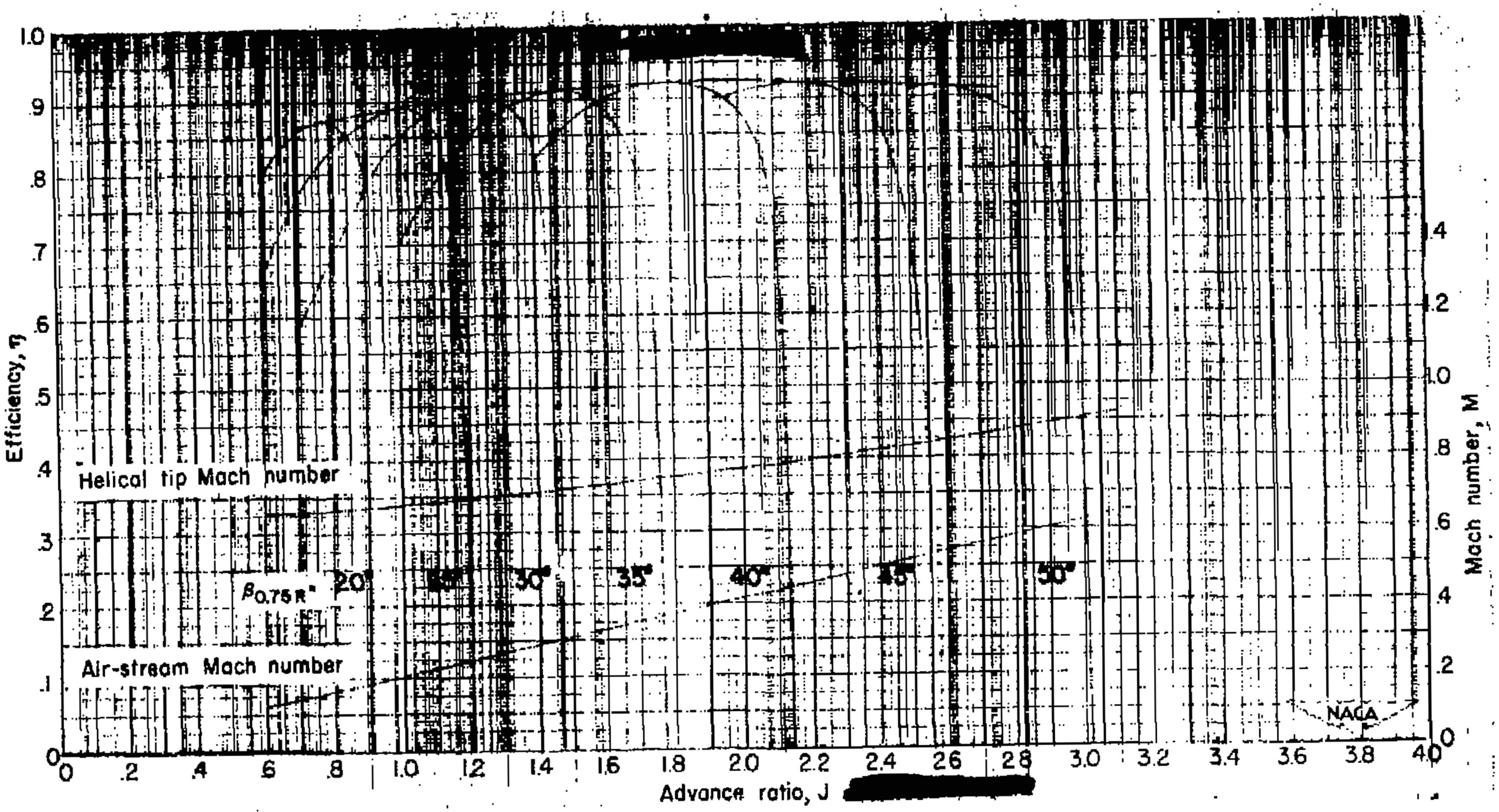

(c) Efficiency.

Figure 4.- Concluded. Rotational speed, 1350 rpm.

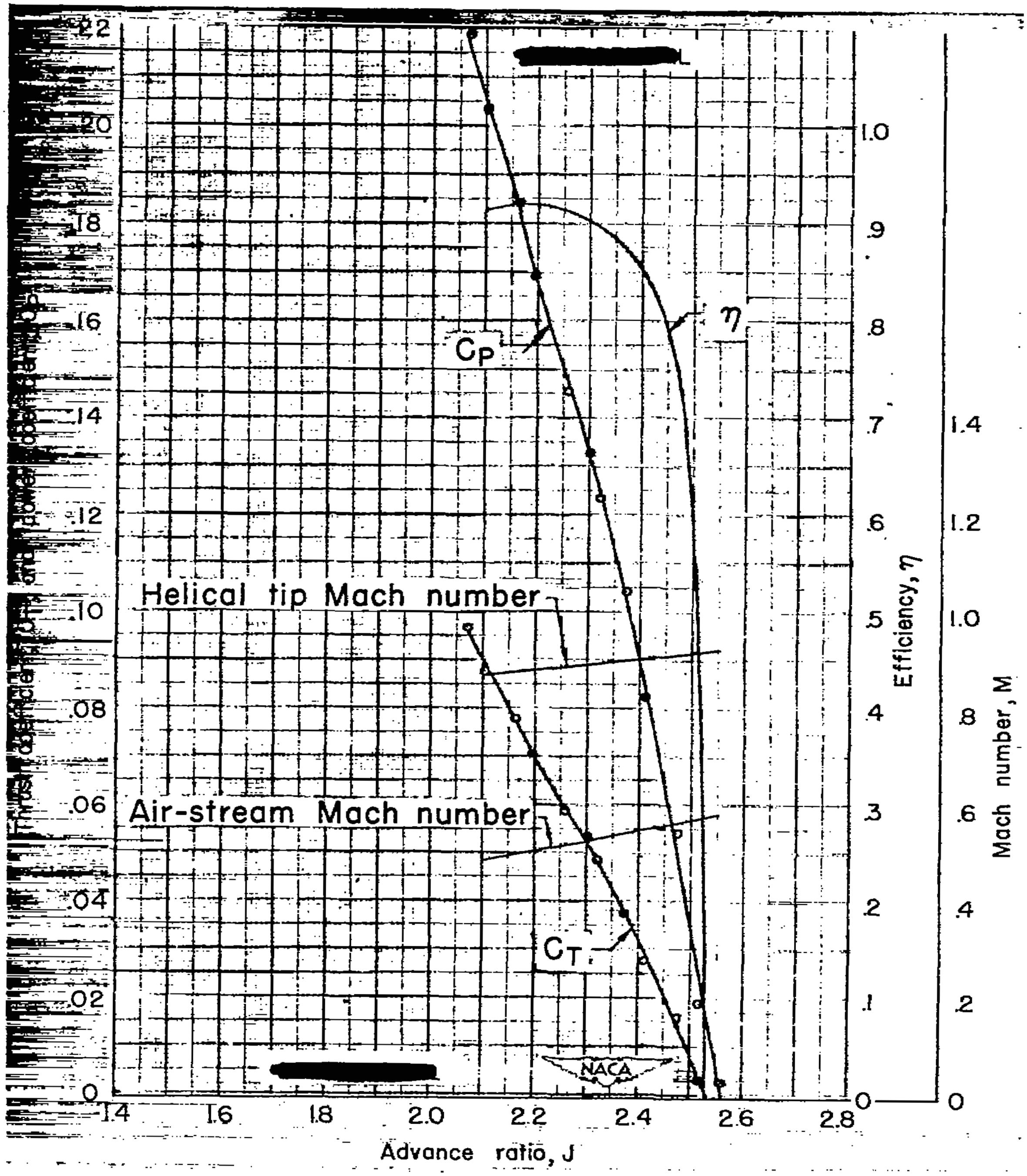

Figure 5.- Characteristics of three-blade propeller with NACA 10-(3)(08)-03 blades. $\beta_{0.75R} = 45^{\circ}$. Rotational speed, 1500 rpm.

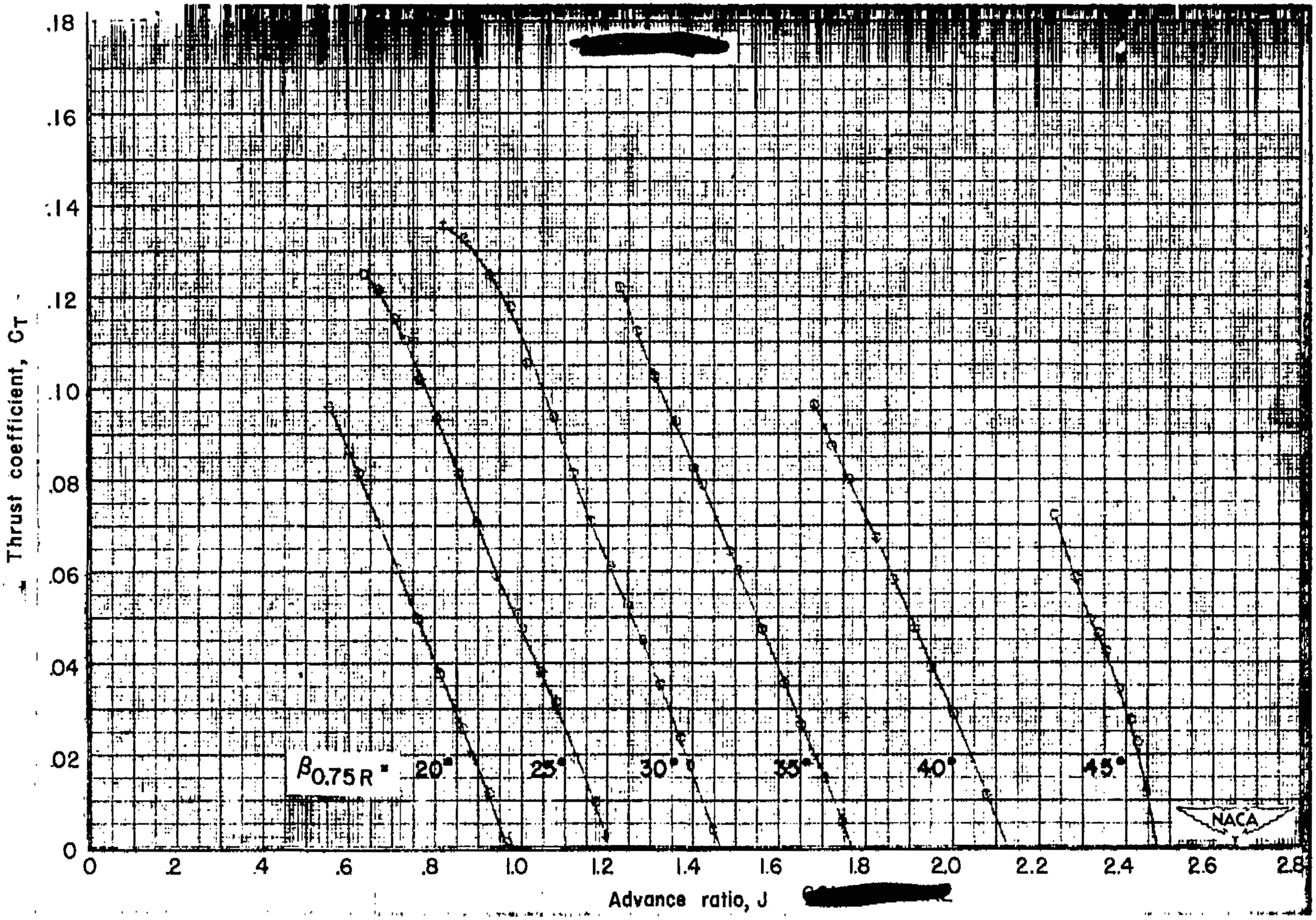

(a) Thrust coefficient.

Figure 6.- Characteristics of three-blade propeller with NACA 10-(3)(08)-03 blades. Rotational speed, 1600 rpm.

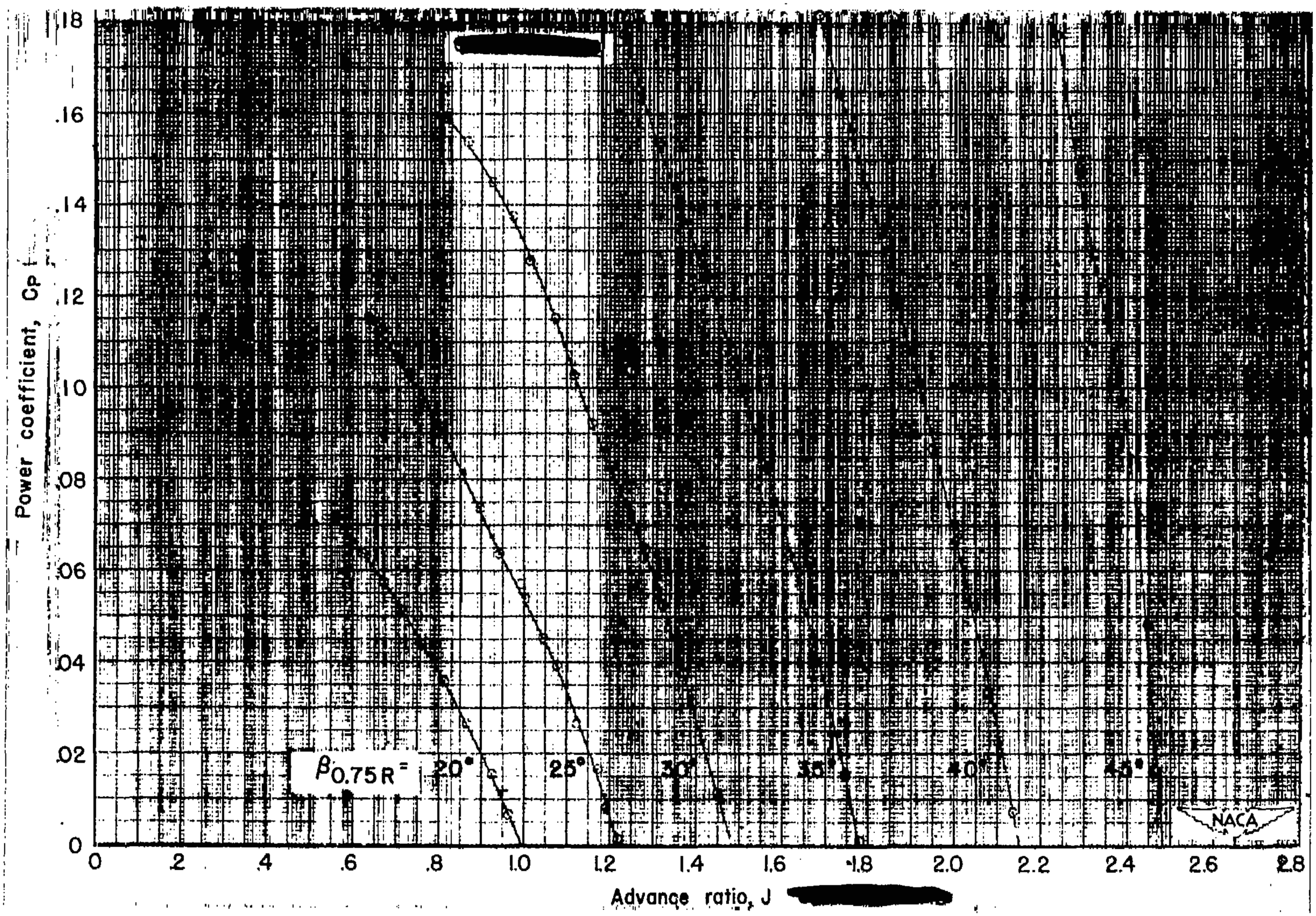

(b) Power coefficient.

Figure 6.- Continued. Rotational speed, 1600 rpm.

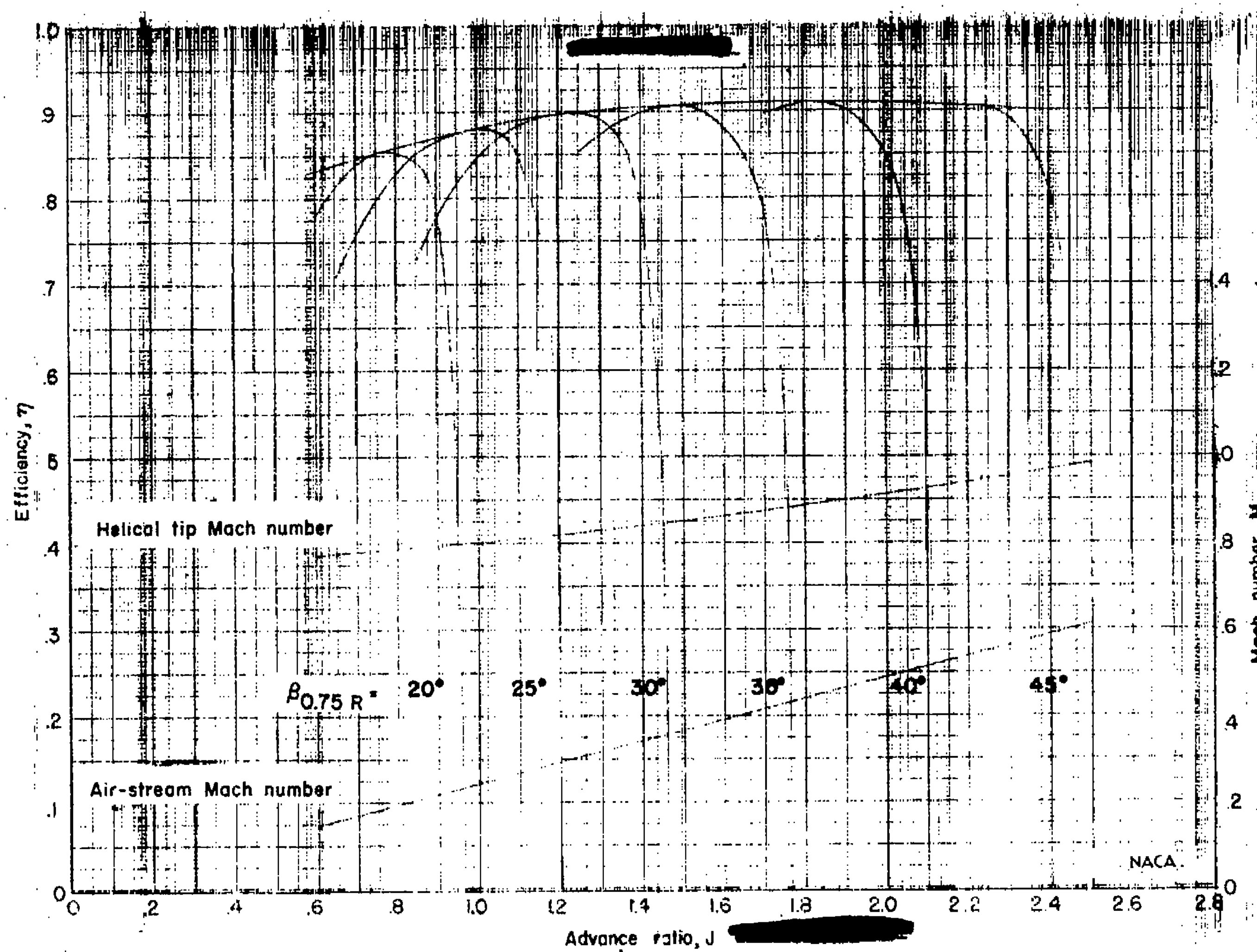

(c) Efficiency.

Figure 6.- Concluded. Rotational speed, 1600 rpm.

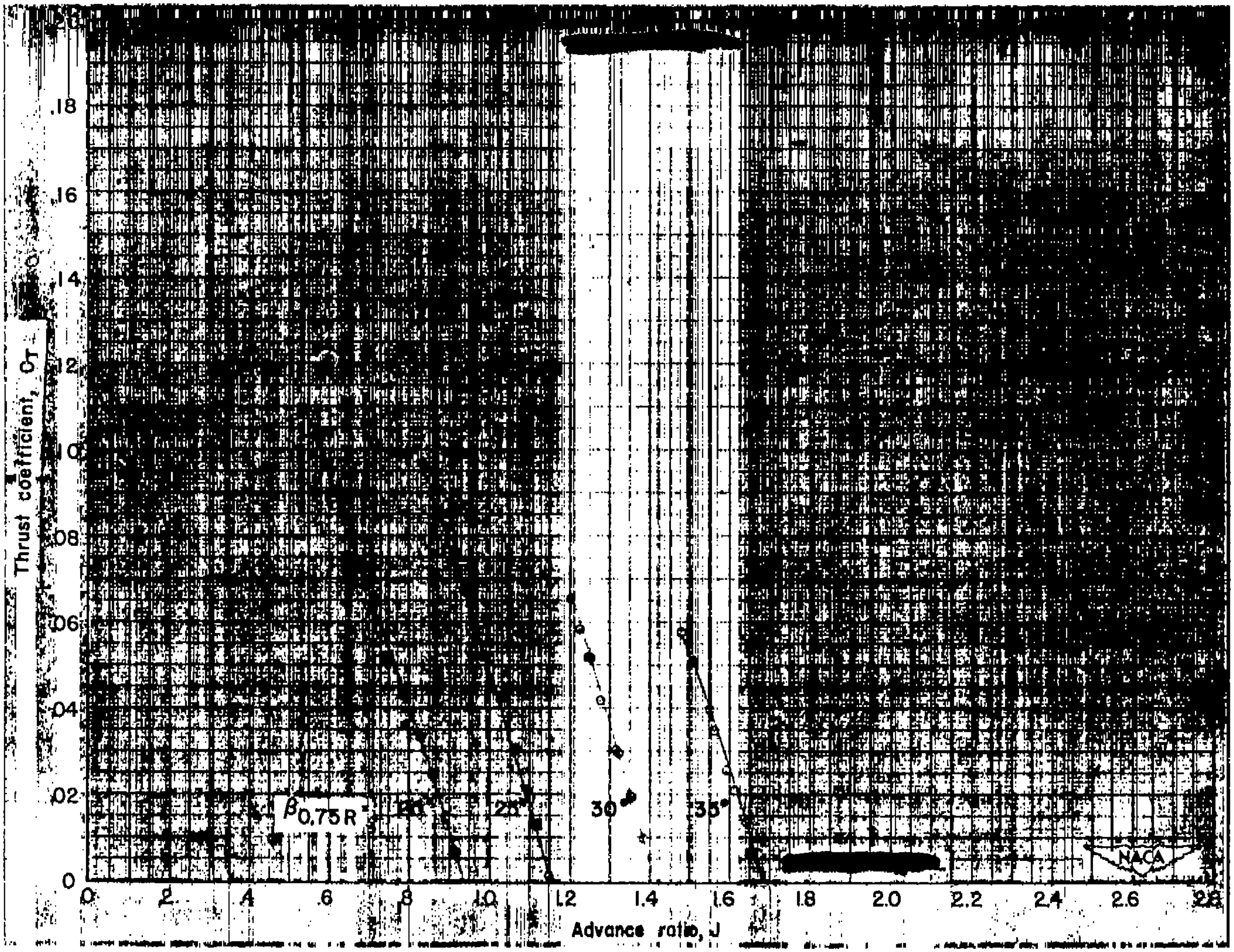

(a) Thrust coefficient.

Figure 7.- Characteristics of three-blade propeller with NACA 10-(3)(08)-03 blades. Rotational speed, 2000 rpm.

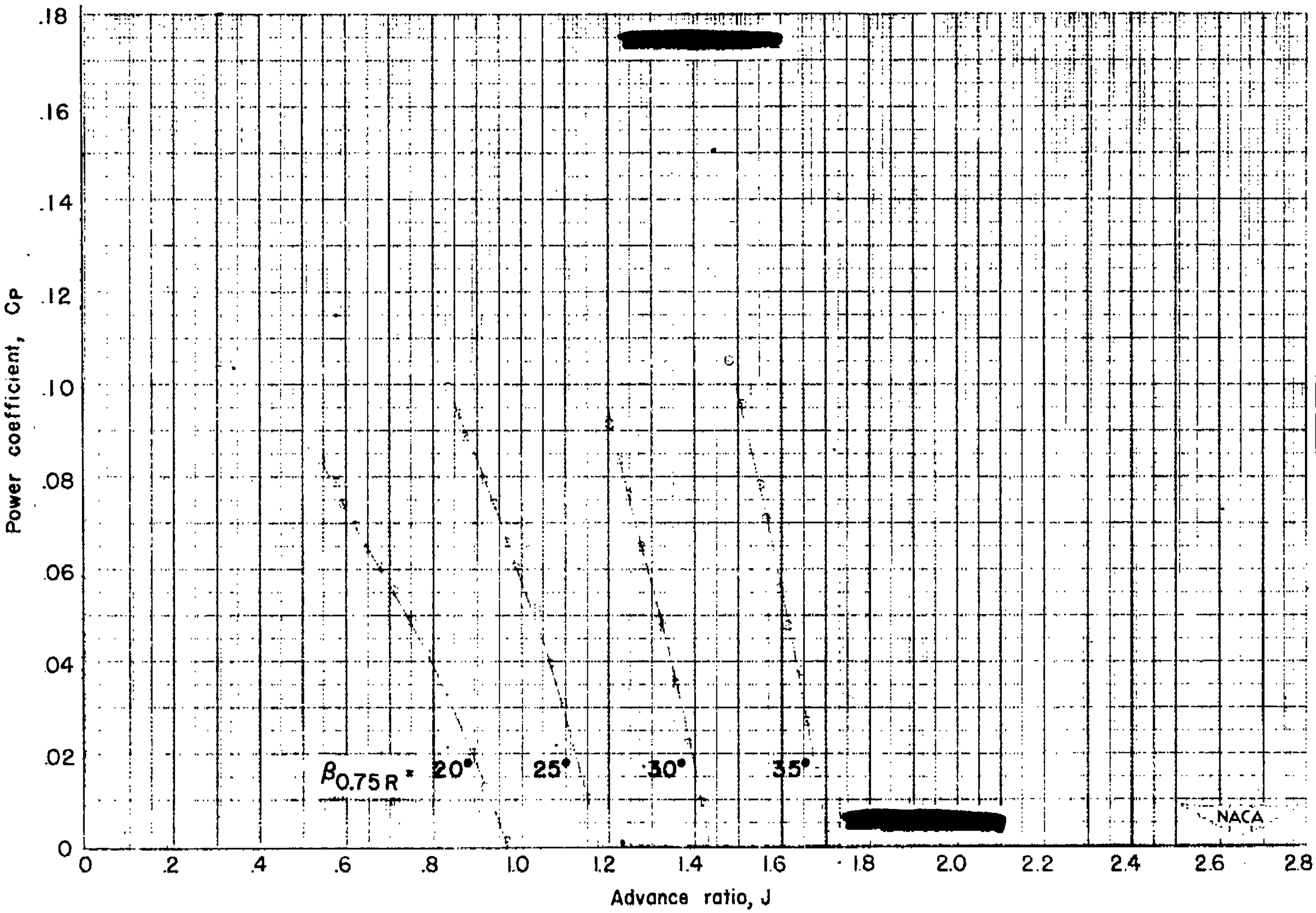

(b) Power coefficient.

Figure 7.- Continued. Rotational speed, 2000 rpm.

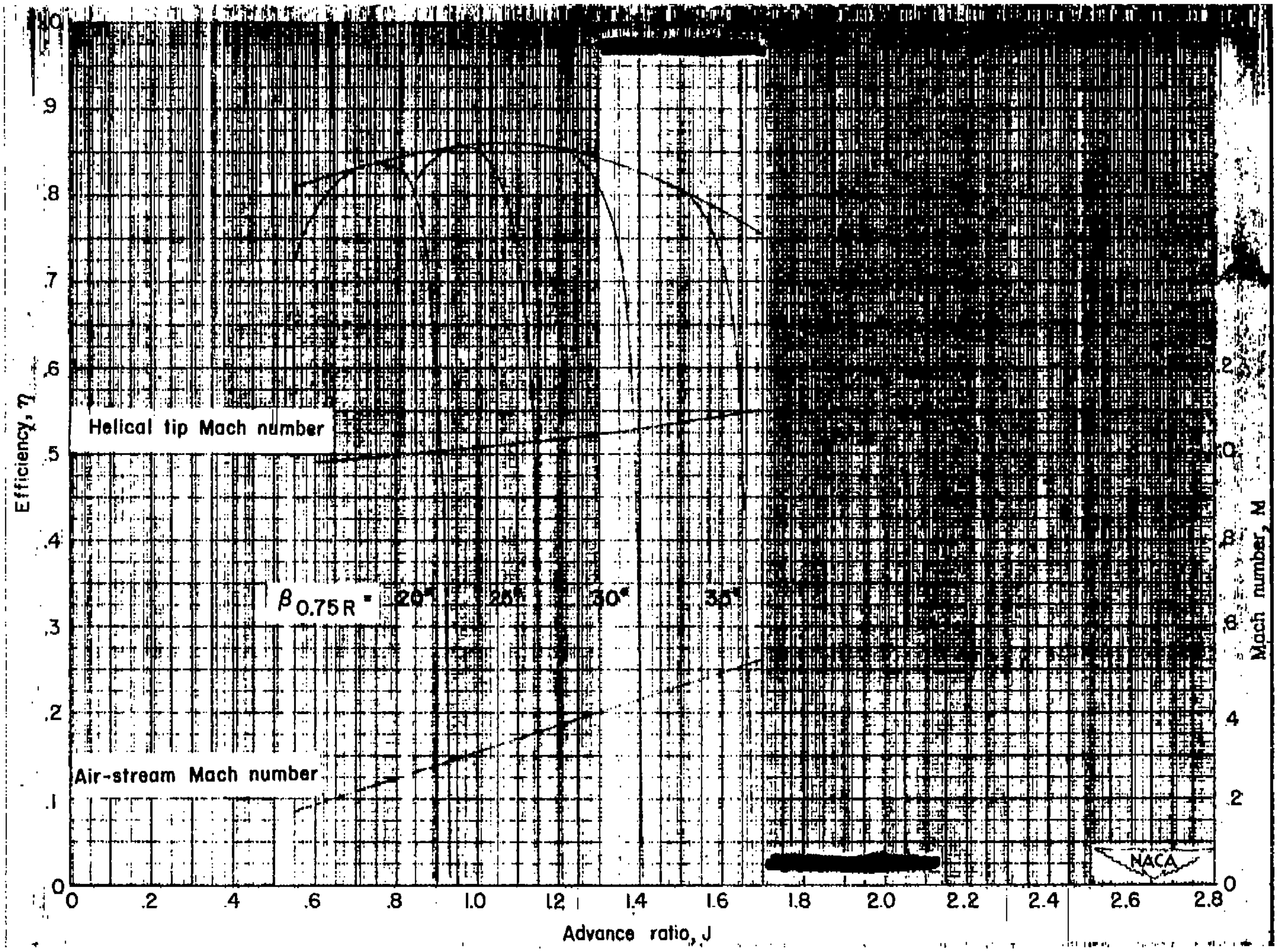

(c) Efficiency.

Figure 7.- Concluded. Rotational speed, 2000 rpm.

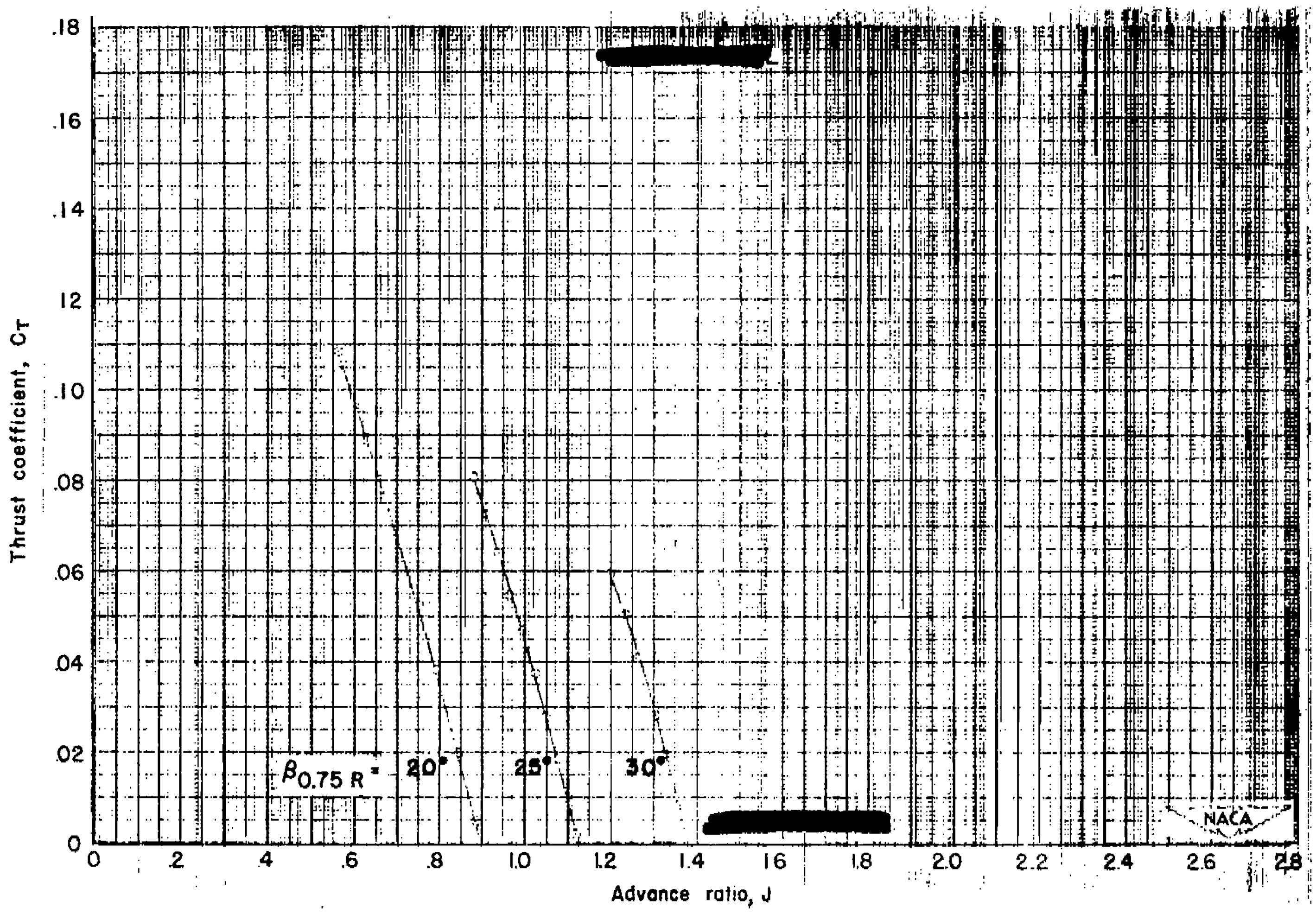

(a) Thrust coefficient.

Figure 8.- Characteristics of three-blade propeller with NACA 10-(3)(08)-03 blades. Rotational speed, 2160 rpm.

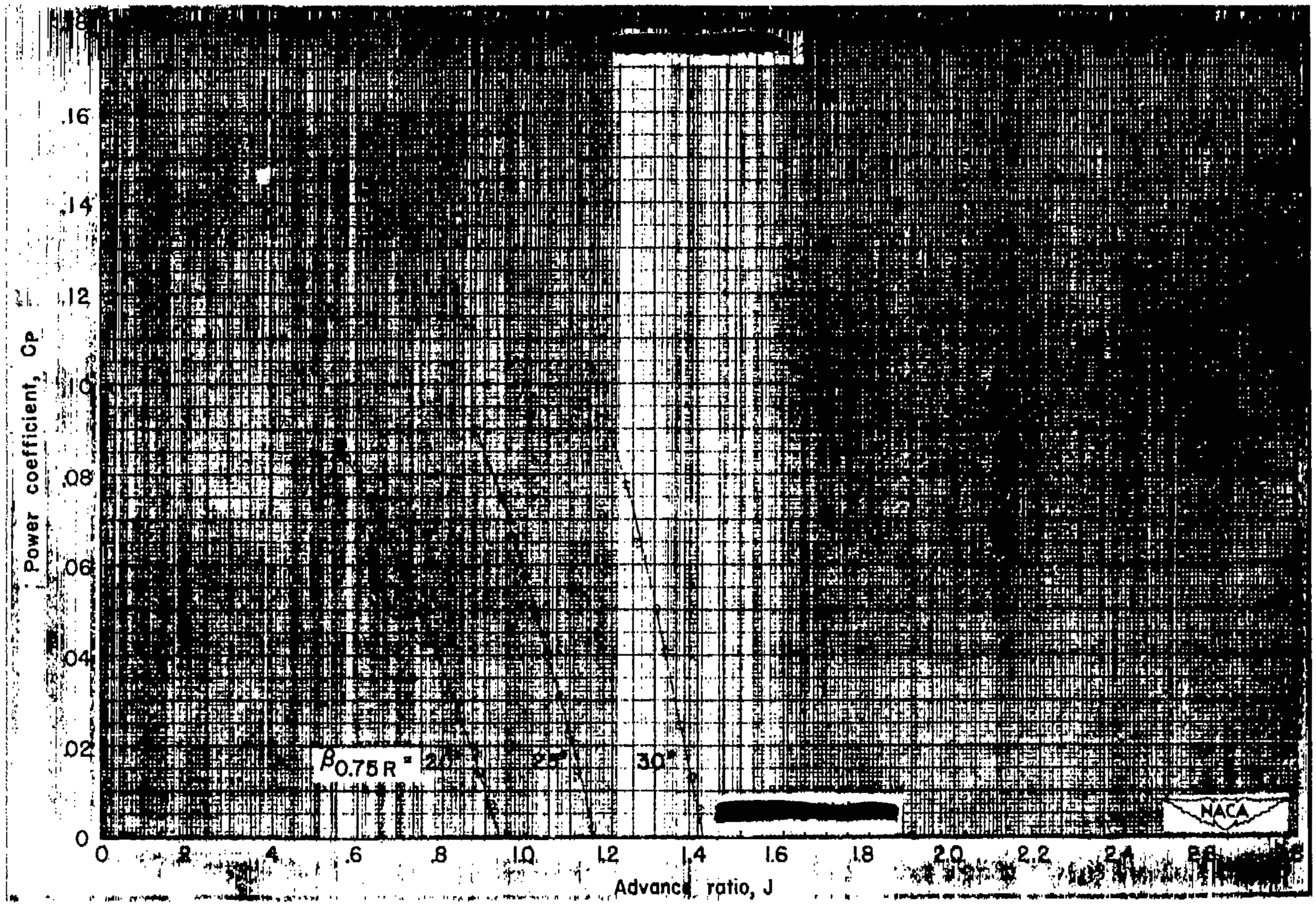

(b) Power coefficient.

Figure 8.- Continued. Rotational speed, 2160 rpm.

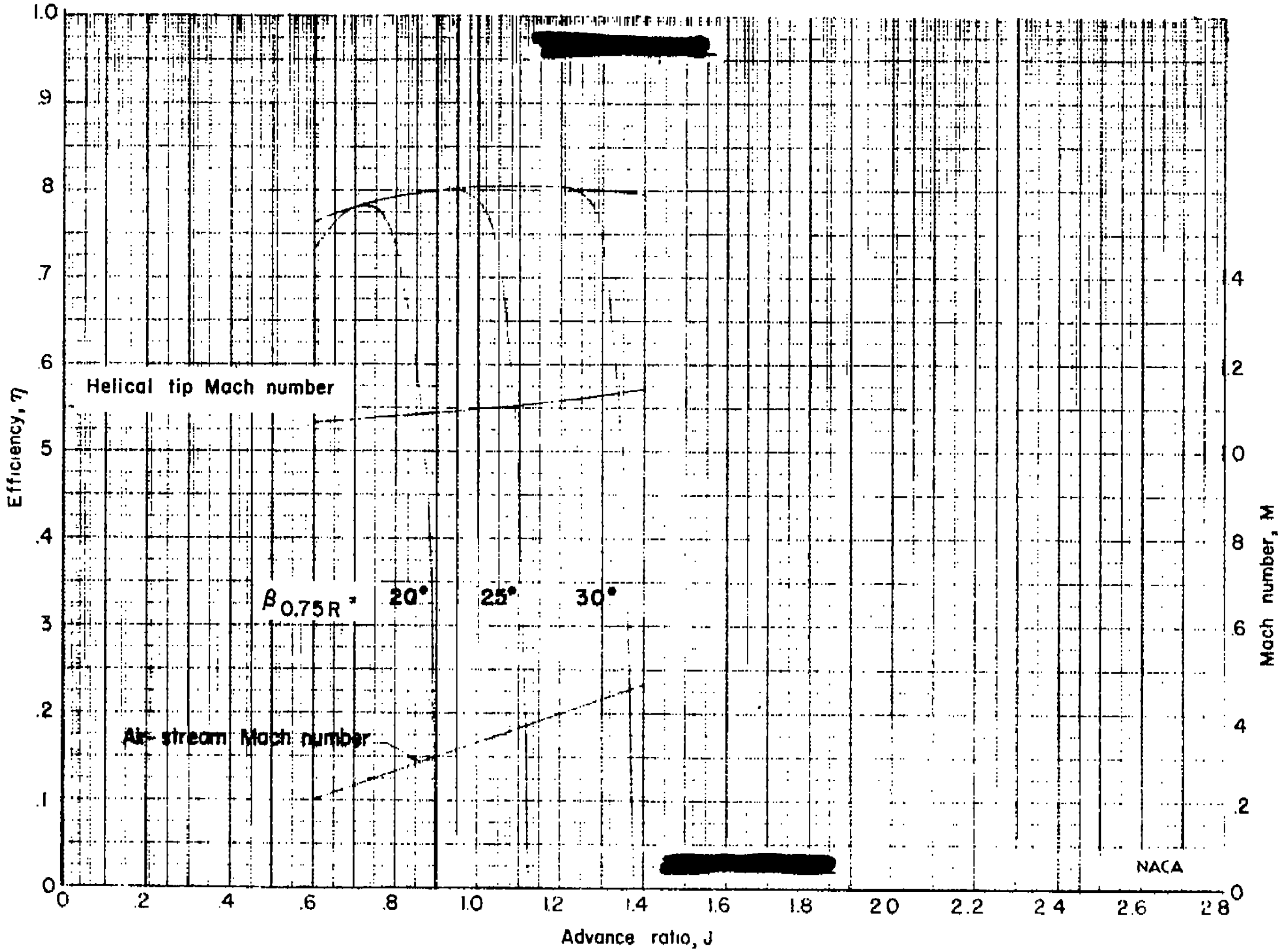

(c) Efficiency.

Figure 8.- Concluded. Rotational speed, 2160 rpm.

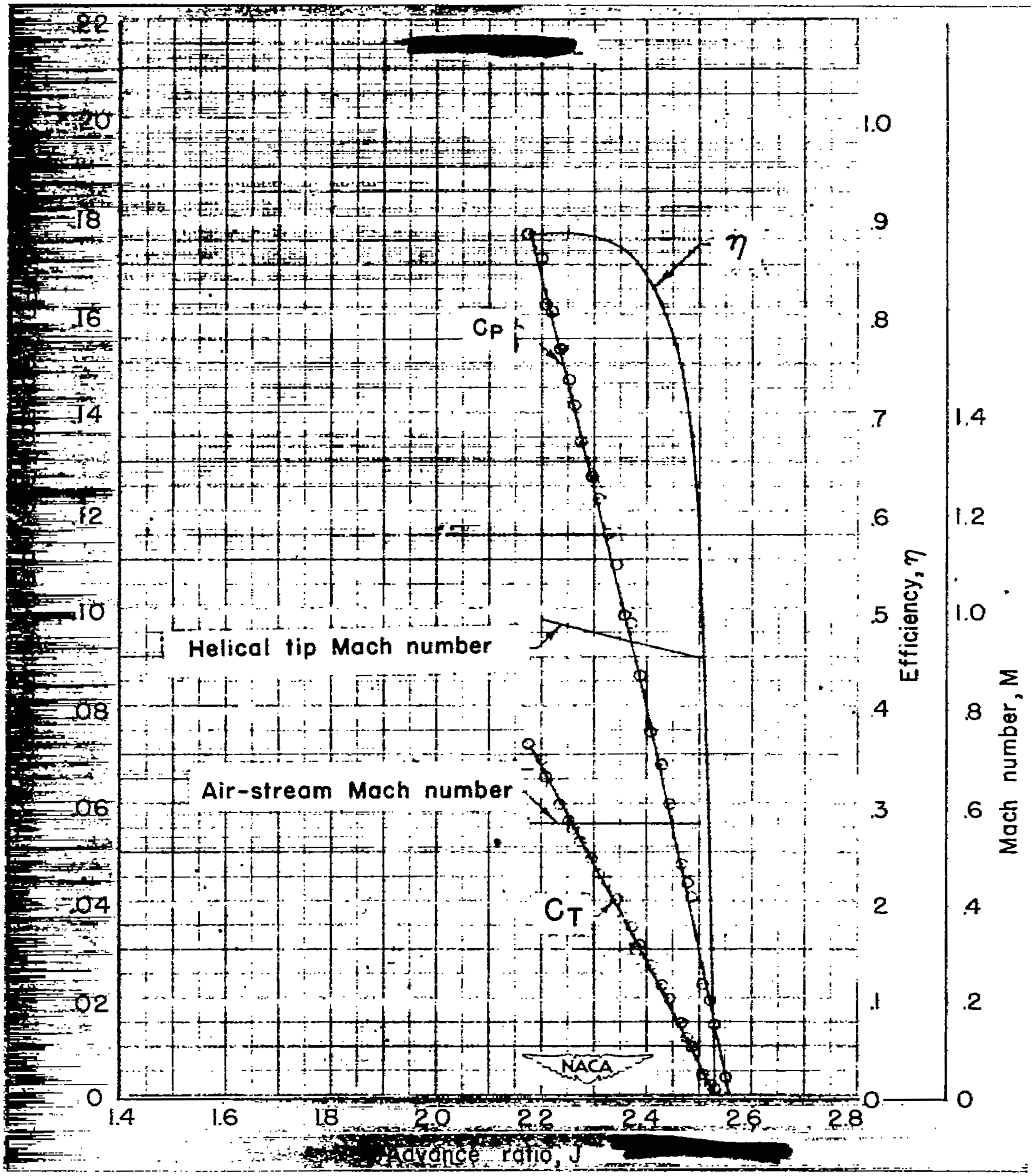

(a) Air-stream Mach number at maximum efficiency, 0.56.

Figure 9.- Characteristics of three-blade propeller with NACA 10-(3)(08)-03 blades at high forward speeds. $\beta_{0.75R} = 45^{\circ}$.

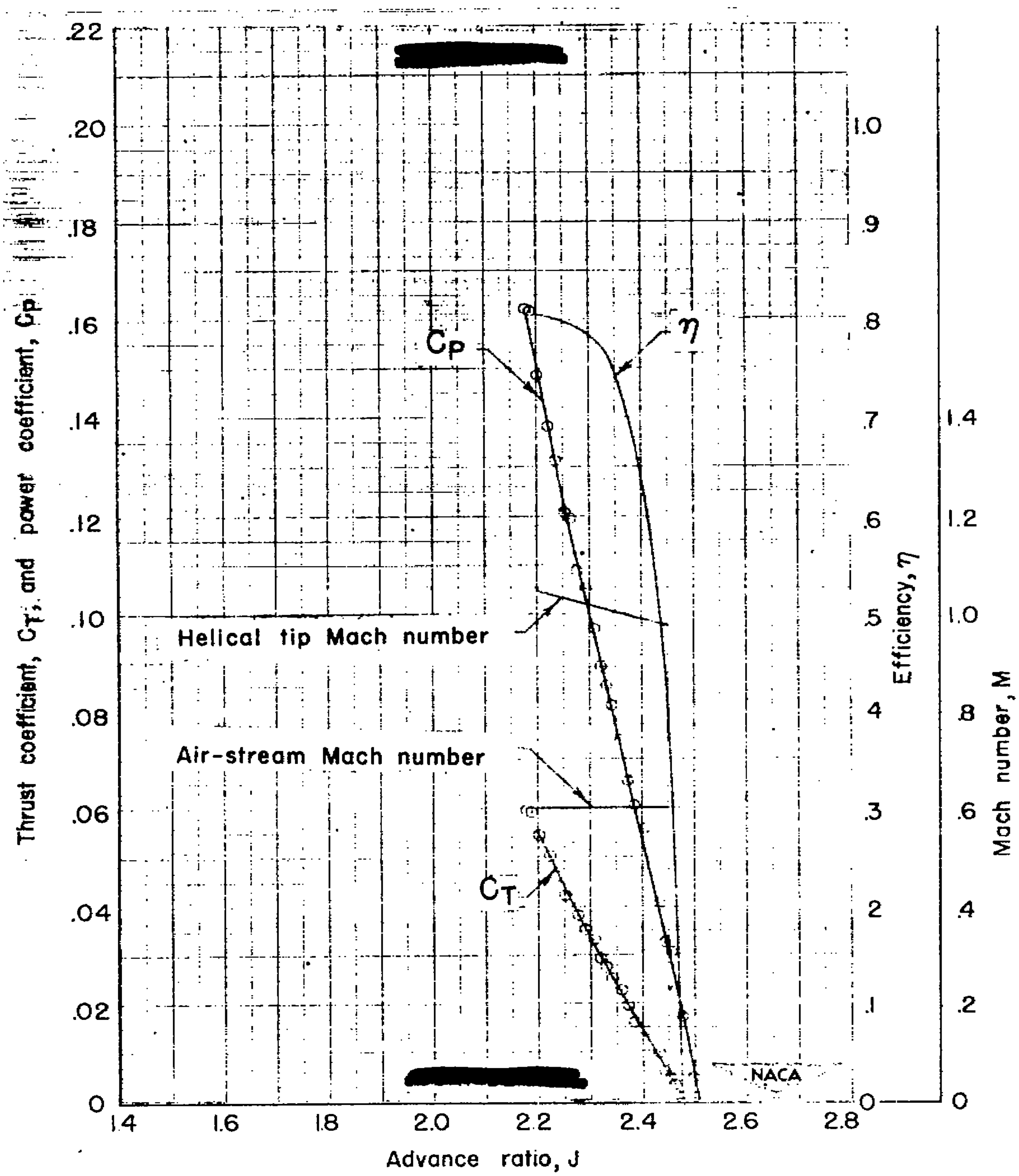

(b) Air-stream Mach number at maximum efficiency, 0.60.

Figure 9.- Continued.

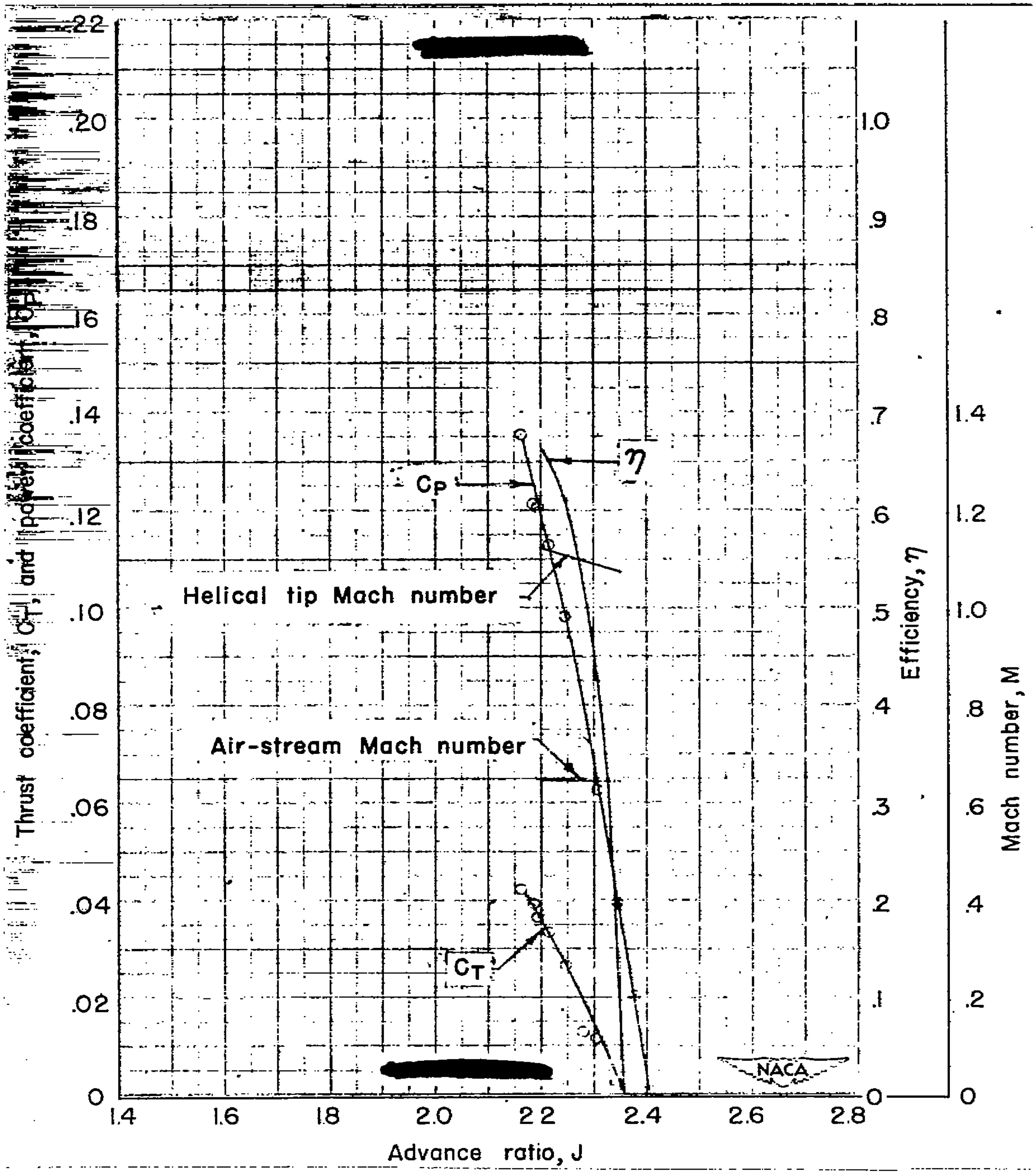

(c) Air-stream Mach number at maximum efficiency, 0.64.

Figure 9.- Concluded.

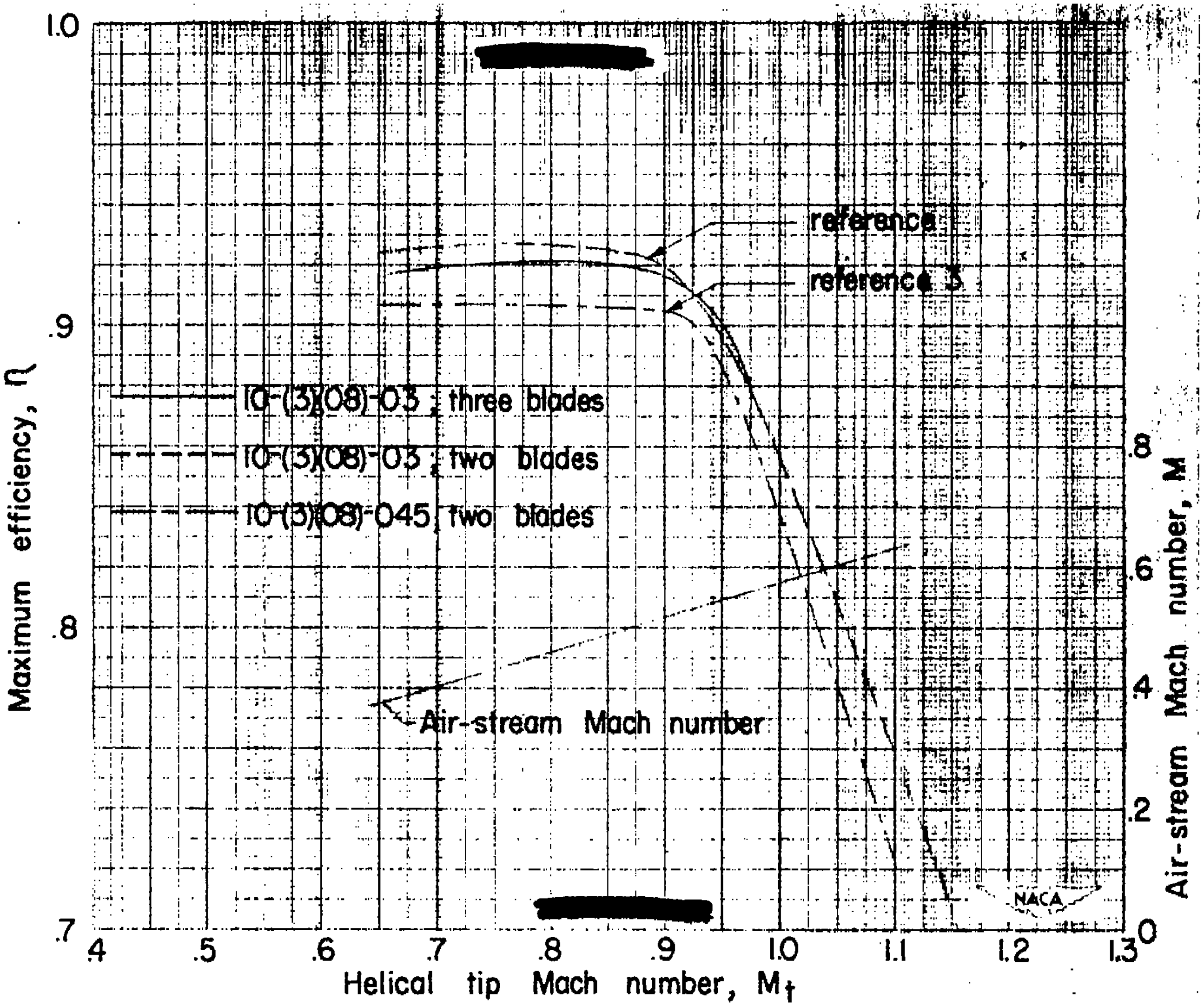

Figure 10.- Effect of compressibility on peak efficiency at design blade angle.

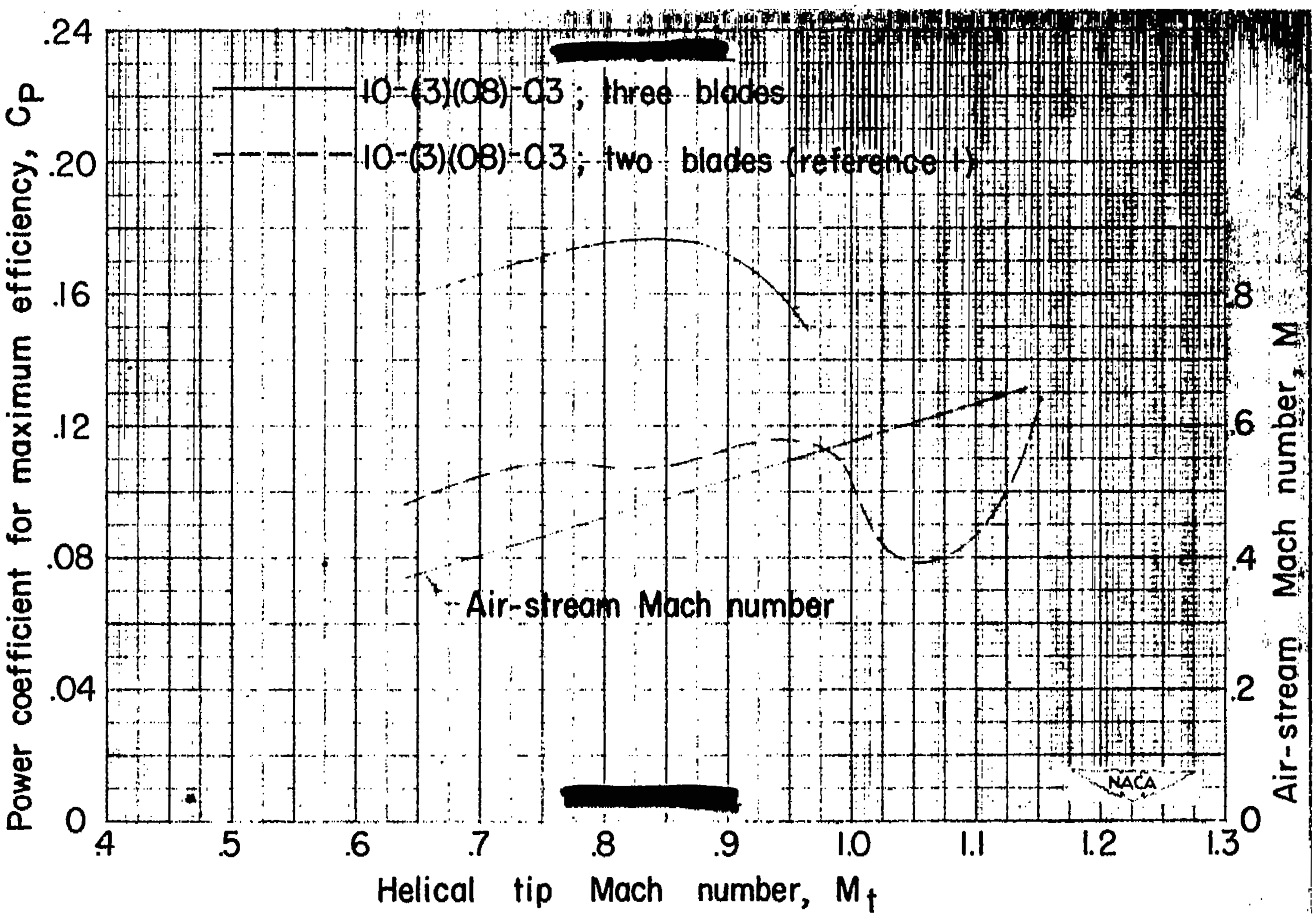

Figure 11.- Effect of compressibility on power coefficient at design blade angle for the three-blade propeller in comparison with the two-blade propeller of reference 1.